BIOCHEMISTRY
including biophysical chemistry & molecular biology

Article

pubs.acs.org/biochemistry

Pseudouridine Monophosphate Glycosidase: A New Glycosidase Mechanism

Siyu Huang,[†] Nilkamal Mahanta,[‡] Tadhg P. Begley,*[,‡] and Steven E. Ealick*[,†]

[†]Department of Chemistry and Chemical Biology, Cornell University, Ithaca, New York 14853, United States

[‡]Department of Chemistry, Texas A&M University, College Station, Texas 77843, United States

Supporting Information

ABSTRACT: Pseudouridine (Ψ), the most abundant modification in RNA, is synthesized in situ using Ψ synthase. Recently, a pathway for the degradation of Ψ was described [Preumont, A., Snoussi, K., Stroobant, V., Collet, J. F., and Van Schaftingen, E. (2008) *J. Biol. Chem. 283*, 25238−25246]. In this pathway, Ψ is first converted to Ψ 5′-monophosphate (ΨMP) by Ψ kinase and then ΨMP is degraded by ΨMP glycosidase to uracil and ribose 5-phosphate. ΨMP glycosidase is the first example of a mechanistically characterized enzyme that cleaves a C−C glycosidic bond. Here we report X-ray crystal structures of *Escherichia coli* ΨMP glycosidase and a complex of the K166A mutant with ΨMP. We also report the structures of a ring-opened ribose 5-phosphate adduct and a ring-opened ribose ΨMP adduct. These structures provide four snapshots along the reaction coordinate. The structural studies suggested that the reaction utilizes a Lys166 adduct during catalysis. Biochemical and mass spectrometry data further confirmed the existence of a lysine adduct. We used site-directed mutagenesis combined with kinetic analysis to identify roles for specific active site residues. Together, these data suggest that ΨMP glycosidase catalyzes the cleavage of the C−C glycosidic bond through a novel ribose ring-opening mechanism.

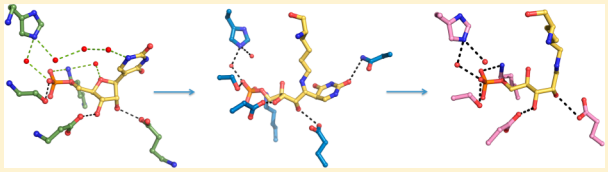

Pseudouridine (Ψ) was the first modified nucleoside to be discovered and is the most abundant modification in RNA, existing in tRNAs, rRNAs, snRNAs, and snoRNAs.[1] Ψ is biosynthesized post-transcriptionally from RNA uridine moieties by Ψ synthase, which cleaves the glycosidic C−N bond and reconnects the uracil to the ribosyl moiety at the C5 position.[2] Pseudouridine reduces the conformational flexibility of RNA because the exposed, protonated N1 atom forms strong hydrogen bonds with structured water molecules, replacing weak interactions formed by C5.[1,3]

While Ψ biosynthesis has been studied extensively, little is known about Ψ catabolism. Recently, the two enzymes responsible for Ψ **1** degradation in *Escherichia coli* were identified.[4] Ψ kinase first phosphorylates Ψ to pseudouridine 5′-phosphate (ΨMP, **2**). ΨMP glycosidase then catalyzes the reversible cleavage of the C−C glycosidic bond to form uracil **4** and ribose 5-phosphate (R5P, **3**) (Scheme 1). While ΨMP glycosidase functions biologically in the cleavage direction, the equilibrium strongly favors ΨMP synthesis with an equilibrium constant for the degradation reaction of 2.3×10^{-4} M.[4] In bacterial genomes, Ψ kinase and ΨMP glycosidase are encoded by separate genes. In *E. coli*, these genes are *yeiC* and *yeiN*, respectively, which are located in the same operon. In some eukaryotes, the genes for Ψ kinase and ΨMP glycosidase are fused, resulting in a bifunctional enzyme. Enzymes metabolizing Ψ are not found in humans and most other higher organisms, and excess Ψ is excreted.[5]

While natural products containing O and N glycosidic bonds are widespread, natural products containing the C glycosidic bond are much less prevalent.[6] The C glycosidic bond is generally thought to be formed by an electrophilic aromatic substitution. Enzymes that cleave C−N glycosidic bonds have been extensively studied. These include nucleoside and nucleotide hydrolases,[7−9] purine and pyrimidine nucleoside phosphorylases,[10] purine and pyrimidine phosphoribosyltransferases,[11,12] and nucleoside deoxyribosyltransferases.[13] In addition, DNA repair enzymes such as endonuclease III function as *N*-glycosylases to excise damaged nucleobases from DNA.[14] Enzymes that cleave C−O glycosidic bonds are widespread in carbohydrate metabolism and have also been extensively studied.[15] Biochemical, biophysical, and genetic studies suggest that these enzymes cleave C−N and C−O glycosidic bonds by a largely dissociative mechanism generating an oxocarbenium ion intermediate. While the genes encoding several C-glycosynthases have been identified and in many cases overexpressed,[16−23] and the structures of ligand free UrdGT2[24,25] and ΨMP glycosidase[26] have been determined, there is currently no example of a mechanistically well-characterized C-glycosidase or glycosynthase.

Here we report a set of *E. coli* ΨMP glycosidase (EcΨMP glycosidase) crystal structures, which provide four snapshots of the reaction coordinate. The structures are the unliganded enzyme, a ΨMP glycosidase−ring-opened R5P adduct, a ΨMP glycosidase−ring-opened ribose ΨMP adduct, and a K166A−ΨMP complex. The structural studies suggested that the reaction involves an intermediate imine with Lys166. This

Received: May 24, 2012
Revised: October 11, 2012
Published: October 15, 2012

   dx.doi.org/10.1021/bi3006829 | *Biochemistry* 2012, 51, 9245−9255

Scheme 1

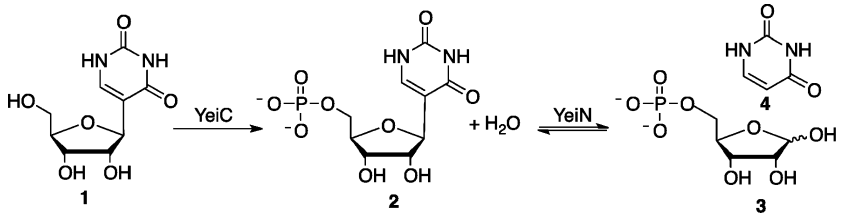

was confirmed by mass spectrometry. Kinetic studies of active site mutants assign roles for individual amino acid side chains. Comparison of the EcΨMP glycosidase structures suggested a role for conformational changes in ΨMP cleavage and product release. These results support an unanticipated mechanism for the pseudouridine glycosidase-catalyzed C glycosyl bond hydrolysis.

MATERIALS AND METHODS

Chemical Reagents. R5P and uracil were purchased from Sigma-Aldrich. Tris(2-carboxyethyl)phosphine (TCEP) was purchased from Hampton Research. Kanamycin was purchased from Acros. Ni-NTA resin was obtained from Qiagen (Valencia, CA).

Cloning, Overexpression, and Purification of ΨMP Glycosidase. Standard methods were used for DNA restriction endonuclease digestion, ligation, and transformation of DNA.[27] Automated DNA sequencing was performed at the Cornell BioResource Center. Plasmid DNA was purified with a GeneJet miniprep kit (Fermentas, Glen Burnei, MD). DNA fragments were separated by agarose gel electrophoresis, excised, and purified with the Zymoclean gel DNA recovery kit (Zymo Research, Orange, CA). *E. coli* strain MachI (Invitrogen, Madison, WI) was used as the recipient for transformations during plasmid construction and for plasmid propagation and storage. An Eppendorf Mastercycler and Phusion DNA polymerase (New England Biolabs, Ipswich, MA) were used for polymerase chain reaction (PCR). All restriction endonucleases and T4 DNA ligase were purchased from New England Biolabs. *E. coli* strain BL21(DE3) and the pET overexpression system were purchased from Novagen (Madison, WI).

The *yeiN* gene was amplified via PCR from *E. coli* K12 genomic DNA using the following primers: upstream primer 5′-GGG TAG CAT ATG TCT GAA TTA AAA ATT TCC CCT G-3′ (inserts an *Nde*I site at the start codon of the *yeiN* open reading frame) and downstream primer 5′-CCC TAC TCG AGT TAA CCC GCG AGA CGC TGA TAT TC-3′ (inserts an *Xho*I site after the end of the *yeiN* open reading frame). The purified PCR product was digested with *Nde*I and *Xho*I, purified, and ligated into similarly digested pTHT, a pET-28-derived vector, which allows attachment of a modified six-histidine tag followed by a tobacco etch virus protease cleavage site onto the N-terminus of the expressed protein. Colonies were screened for the presence of the insert, and a representative plasmid was designated pEcYeiN.THT. The PCR-derived DNA was sequenced and shown to contain no errors.

The *yeiN* gene was further transformed into *E. coli* strain BL21(DE3) (Novagen). The cells were grown overnight in a 10 mL starter culture in Luria-Bertani (LB) medium[28] containing 30 μg/mL kanamycin, then transferred to cultures containing 1.5 L of LB medium, and incubated at 37 °C while being shaken until an OD_{600} of 0.8 was achieved. The culture was then induced with 1 mM isopropyl 1-β-D-galactopyranoside and incubated overnight at 15 °C. Cells were harvested by centrifugation at 10000*g* for 30 min at 4 °C, resuspended in lysis buffer containing 50 mM tris(hydroxymethyl)-aminomethane (Tris) (pH 8.0) 300 mM NaCl, and 10 mM imidazole, and lysed by sonication. The lysate was centrifuged at 40000*g* for 30 min, and the supernatant was loaded onto a column containing 2 mL of Ni-NTA resin (Qiagen) preequilibrated with lysis buffer. The column was then washed with 3 times the volume of wash buffer containing 50 mM Tris (pH 8.0), 300 mM NaCl, and 30 mM imidazole for 1.5 h. The protein was eluted with 50 mM Tris (pH 8.0), 300 mM NaCl, and 250 mM imidazole. The eluted protein was then subjected to size exclusion chromatography using an ACTA Explorer fast-performance liquid chromatography system with a HiLoad 26/60 Superdex 200 prep grade column (GE Healthcare). The resulting protein was more than 95% pure as judged by sodium dodecyl sulfate−polyacrylamide gel electrophoresis analysis (unpublished experiments). The protein was then concentrated to 15 mg/mL using an Amicon concentrator (30 kDa molecular mass cutoff filter, Millipore), flash-frozen, and stored at −80 °C.

ΨMP Glycosidase Mutagenesis. Site-directed mutagenesis was performed by a standard PCR protocol using P*fu*UltraII DNA polymerase per the manufacturer's instructions (Agilent) and *Dpn*I to digest the methylated parental DNA prior to transformation. In addition to the forward and reverse primers required to introduce the mutation, a third primer was designed to screen for the presence of the mutation by colony PCR (Table 1 of the Supporting Information). For screening, the primers designated "sF" were paired with the T7T primer (5′-GCTAGTTATTGCTCAGCGG-3′) and the primers designated "sR" were screened with the T7Plac primer (5′-TATAGGGGAATTGTGAGCGG-3′). All the mutants were verified by sequencing.

Enzymatic Synthesis of ΨMP. ΨMP glycosidase (2.5 mg), uracil (100 mM), and R5P were incubated in a buffer containing 0.5 mM $MnCl_2$ and 25 mM HEPES (pH 7.1) at 25 °C for 1 h. The enzyme was removed using an Amicon 30 kDa molecular mass cutoff (Millipore) filter. The reaction product was identified as ΨMP by comigration with an authentic sample of ΨMP during high-performance liquid chromatography (HPLC) analysis.

Crystallization of ΨMP Glycosidase. ΨMP glycosidase was crystallized using the hanging drop vapor diffusion method at 22 °C. The initial crystallization condition was determined using sparse matrix screens Crystal Screen 1 and 2 (Hampton Research). The optimized reservoir conditions included 20% polyethylene glycol 4000, 0.2 M sodium acetate, and 0.1 M Tris (pH 7.0). ΨMP glycosidase was incubated with 4 mM $MnSO_4$ before crystallization. The drops contained 1.5 μL of a protein

dx.doi.org/10.1021/bi3006829 | *Biochemistry* 2012, 51, 9245−9255

Table 1. Data Collection and Refinement Statistics[a]

	ΨMP glycosidase	ΨMP glycosidase−ring-opened R5P	ΨMP glycosidase−ring-opened ribose ΨMP	K166A−ΨMP
beamline	APS 24-ID-C	APS 24-ID-C	APS 24-ID-C	CHESS F1
wavelength (Å)	0.9792	0.9795	0.9795	0.9180
space group	$P2_12_12_1$	$P2_12_12_1$	$P2_12_12_1$	$P2_12_12_1$
a (Å)	62.1	61.3	61.5	60.7
b (Å)	115.4	116.5	77.1	76.4
c (Å)	132.0	132.2	200.0	199.0
no. of chains per asymmetric unit	3	3	3	3
resolution (Å)	43.5−2.0 (1.94−1.96)	41.2−2.2 (2.19−2.32)	48.1−2.5 (2.50−2.57)	35.3−1.8 (1.80−1.82)
total no. of reflections	404995	196780	124598	422749
no. of unique reflections	70995	49316	33815	86433
redundancy	5.7 (5.5)	4.0 (4.0)	3.7 (3.4)	4.9 (4.9)
R_{merge} (%)[b]	5.5 (34.3)	6.0 (40.9)	7.5 (44.1)	7.3 (43.1)
$I/\sigma(I)$	25.1 (4.2)	17.6 (2.4)	17.5 (3.1)	20.4 (3.6)
no. of reflections in working set	66972	45946	31542	81618
completeness (%)	99.7 (99.6)	99.8 (99.9)	99.1 (96.9)	99.1(100)
R_{work}/R_{free}[c] (%)	18.5/22.0	17.9/23.1	18.5/26.1	17.7/20.7
no. of protein atoms	6404	6528	6378	6573
no. of ligand atoms	18	69	93	66
no. of water atoms	365	340	207	643
average *B* factor for protein (Å^2)	35.0	41.4	53.5	27.3
average *B* factor for water (Å^2)	34.1	37.3	39.9	31.3
average *B* factor for ligand (Å^2)	57.7	39.5	49.5	17.6
rmsd for bonds (Å)	0.008	0.007	0.008	0.007
rmsd for angles (deg)	1.2	1.2	1.3	1.2

[a]Values in parentheses are for the highest-resolution shell. [b]$R_{merge} = \sum\sum_i|I_i - \langle I\rangle|/\sum\langle I\rangle$, where $\langle I\rangle$ is the mean intensity of the *N* reflections with intensities I_i and common indices *h*, *k*, *l*. [c]$R = \sum_{hkl}||F_{obs}| - k|F_{cal}||/\sum_{hkl}|F_{obs}|$, where F_{obs} and F_{cal} are observed and calculated structure factors, respectively. R_{work} is calculated over all reflections used in the refinement. R_{free} is calculated over a subset of reflections (5%) excluded from all stages of refinement.

solution and 1.5 μL of a reservoir solution. Prismatic crystals grew within 2 days to a size of 200 μm × 50 μm × 50 μm.

The ΨMP glycosidase−R5P complex was cocrystallized under similar conditions except that the protein was incubated with 4 mM $MnCl_2$ and 2 mM R5P for 30 min prior to crystallization. The ΨMP glycosidase−ring-opened ribose ΨMP complex was obtained by cocrystallizing ΨMP glycosidase with 4 mM $MnCl_2$, 2 mM R5P, and saturated uracil. The K166A−ΨMP complex was prepared by cocrystallizing the mutant enzyme with R5P and uracil.

Data Collection and Processing. Prior to data collection, crystals were soaked in a cryoprotectant solution of 5% glycerol in mother liquor to avoid damage during vitrification. Data sets for ΨMP glycosidase and the complexes were collected at Northeast Collaborative Access Team (NE-CAT) beamline 24-ID-C at the Advanced Photon Source (APS) using an ADSC Quantum 315 detector (Area Detector Systems Corp.) at a wavelength of 0.9795 Å with 1 s exposure times and 1° oscillation angles. The data set for the K166A−ΨMP complex was collected at Cornell High Energy Synchrotron Source (CHESS) using an ADSC Quantum 270 detector at a wavelength of 0.9180 Å with 1 s exposure times and 1° oscillation angles. The detector distances were 275, 350, 325, and 200 cm for the ΨMP glycosidase, the R5P complex, the ring-opened ribose ΨMP complex, and the K166A−ΨMP complex, respectively. Data were indexed, integrated, and scaled using the HKL2000 program suite.[29] Data collection statistics are summarized in Table 1.

Structure Determination and Refinement. The structure of EcΨMP glycosidase was determined by molecular replacement using MOLREP.[30] The search model was a monomer of Protein Data Bank (PDB) entry 1VKM, which has a sequence 39% identical to that of ΨMP glycosidase, after modification by CHAINSAW.[31] 1VKM was originally reported to be an indigoidine (IndA)-like protein from *Thermotoga maritima*[26] but later was shown to be a ΨMP glycosidase.[4] The model was refined through successive rounds of manual model building using COOT[32] and restrained refinement with REFMAC5.[33] Water molecules were then included after the model converged, followed by two additional rounds of refinement. The structure of the ΨMP glycosidase−ring-opened R5P adduct was determined by using the structure of unliganded ΨMP glycosidase as the model and refining with PHENIX.[34] The structure of the ΨMP glycosidase−ring-opened ribose ΨMP adduct, which crystallized in a different space group, was determined by molecular replacement using MOLREP[30] using a monomer from the refined ΨMP glycosidase as the search model. The structure of the K166A−ΨMP complex was determined by using the structure of the ΨMP glycosidase−ring-opened ribose ΨMP adduct as the model and refining with PHENIX.[34] The ligand contents and alternative side chain conformations were determined by $F_{obs} - F_{cal}$ maps and composite omit maps from PHENIX.[34] All ligands were clearly observed in the composite omit map but were not placed until the last stage of the refinement. The final refinement statistics are summarized in Table 1.

dx.doi.org/10.1021/bi3006829 | *Biochemistry* 2012, 51, 9245−9255

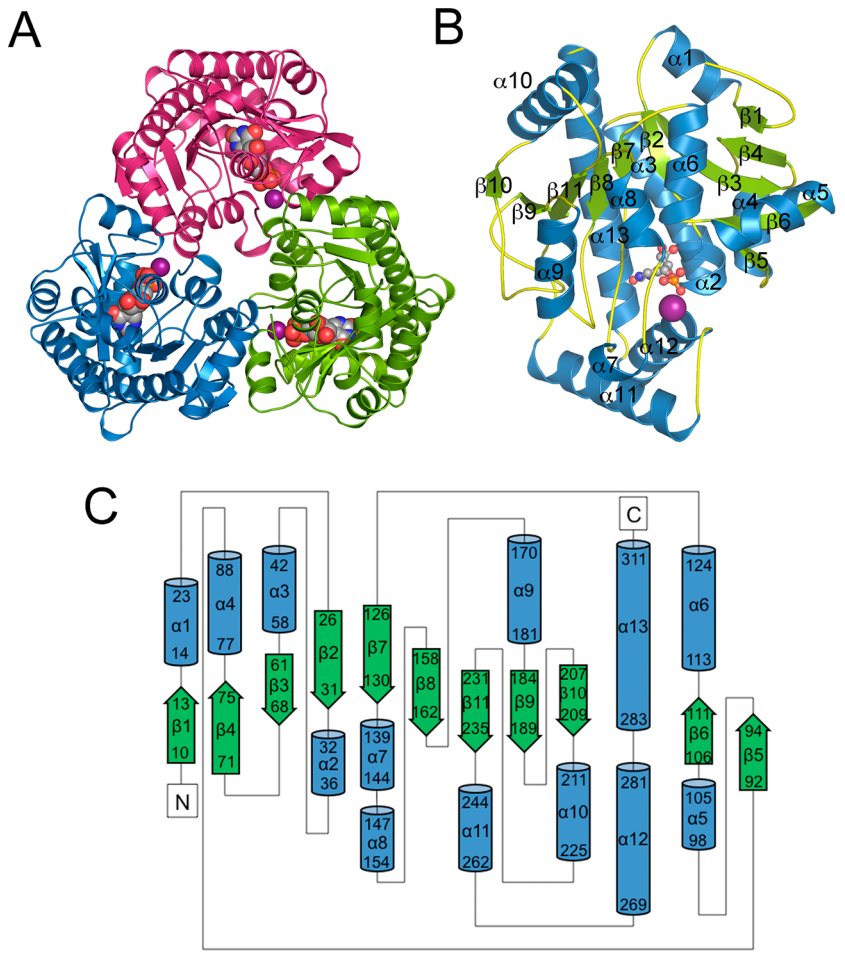

Figure 1. Structure of ΨMP glycosidase. (A) Ribbon diagram of the ΨMP glycosidase trimer color-coded by protomer. The active site is indicated by the space filling model. The Mn(II) ion is colored purple. (B) Ribbon diagram of a ΨMP glycosidase protomer labeled with color-coded α-helices (blue) and β-strands (green). (C) Topology diagram of ΨMP glycosidase. The green arrows represent β-strands and blue cylinders α-helices. The first residue number and the last residue number of each secondary structural element are indicated.

HLPC Analysis of the Reaction Mixture. HPLC analysis following a linear gradient, at a flow rate of 1 mL/min, was used with absorbance detection at 254 nm. Solvent A was water; solvent B was 100 mM K_2HPO_4 (pH 6.6), and solvent C was methanol: 100% B at 0 min, 10% A and 90% B at 5 min, 25% A, 60% B, and 15% C at 7 min, 25% A, 60% B, and 15% C at 17 min, 30% A, 40% B, and 30% C at 19 min, 100% B at 21 min, and 100% B at 30 min. The column used was a Supelcosil LC-18-T HPLC column (15 cm × 4.6 mm, 3 μm particle size).

Determination of k_{cat} and K_m for the Reverse ΨMP Glycosidase Reaction. Uracil concentrations were varied while the R5P concentration was kept at saturation (1 mM) and the Mn(II) concentration at 250 μM. ΨMP formation was monitored by HPLC analysis. Each reaction mixture was divided into 90 μL aliquots, and 10 μL of 10 μM ΨMP glycosidase was added to achieve the final concentration of 1 μM. For each set of reactions, the reaction was quenched at 20 s, 40 s, 1 min, 2 min, 3 min, 5 min, and 10 min time points when the mixture was heated at 100 °C for 2 min. In the case of K166A, the uracil concentrations were varied while the R5P concentration was kept at 1 mM and the Mn(II) concentration at 250 μM for five different sets of reactions. Each reaction mixture was divided into 85 μL aliquots, and 15 μL of 250 μM K166A was added to start the reaction (final concentration of 37.5 μM). For each set of reactions, the reaction was quenched at 20 s, 40 s, 1 min, 2 min, 3 min, 5 min, and 10 min time points when the mixture was heated at 100 °C for 2 min. All samples were analyzed by HPLC, and the amount of ΨMP formed was plotted against time for each set of substrate concentrations. The initial slopes from each set of reactions were then plotted against the substrate concentration and fit to the Michaelis–Menten equation using KaleidaGraph (Synergy Software). The mutant E31A, K93A, H137A, D149A, and N289A activities were measured using a similar procedure.

Biochemical Characterization of the ΨMP Glycosidase R5P Adduct. A reaction mixture containing 2 mM R5P and 1 mM Mn(II) in 50 mM Tris-HCl, 100 mM NaCl, and 2 mM TCEP (pH 8.0) was incubated at room temperature for 1 h with ΨMP glycosidase (50 μM), followed by addition of sodium borohydride (2 mg) and further incubation at room temperature for 45 min. The sample was then buffer-exchanged into 10 mM ammonium acetate (pH 8.0) using a Bio-Rad desalting column and analyzed by ICR-MS. Control samples, one containing 2 mM uracil and the other lacking R5P and Mn(II), were similarly prepared and analyzed.

To locate the site of adduct formation, trypsin digestion analysis was performed on each of these samples as follows. Ten microliters of guanidine hydrochloride (6 M) was added to each sample (50 μL containing 100 μg of ΨMP glycosidase), followed by 1 μL of DTT (200 mM). After a 1 h incubation at

dx.doi.org/10.1021/bi3006829 | Biochemistry 2012, 51, 9245–9255

room temperature, 10 μL of iodoacetamide (200 mM) was added, and the reaction mixture was further incubated in the dark for 1 h. Twenty-nine microliters of ammonium bicarbonate buffer was further added to reduce the final concentration of guanidine hydrochloride to 0.6 M (final volume of 100 μL). One microliter of trypsin in 50 mM ammonium bicarbonate buffer (pH 8.0, 1 μg/ μL) was added, and the samples were incubated at 37 °C for 20 h. The samples were then analyzed by liquid chromatography and mass spectrometry.

RESULTS

Overall Structure of ΨMP Glycosidase. ΨMP glycosidase is a homotrimer (Figure 1A) with one trimer per asymmetric unit in the crystal structure. Of the 312 possible residues, each protomer is complete except for the first two to five residues at the N-terminus and the C-terminal residue, which is missing in most of the protomers. ΨMP glycosidase shows an $\alpha\beta\alpha$ fold. The central mixed β-sheet contains 11 strands with a 1↑4↑3↓2↓7↓8↓11↓9↓10↓5↑6↑ topology and is flanked by six α-helices on one side and seven α-helices on the other (Figure 1B,C). The structure of the protomer is similar to that of PDB entry 1VKM,[26] which was used as a search model during molecular replacement. The trimer contains a buried surface area of 8650 Å^2, accounting for 27.8% of the total surface area. The trimer interface is formed primarily by helices α5 and α8 from one protomer and helices α9 and α10 from the adjacent protomer. The interface includes hydrogen bonds between Ile146 and Thr180* (an asterisk indicates residues from an adjacent protomer) and between Arg96 and Asn228*, and a salt bridge between Arg97 and Glu179*.

Mn(II) Binding Site. Mn(II) is required for ΨMP glycosidase activity[4] and for the formation of high-quality crystals. The Mn(II) coordination is octahedral with Mn(II)−oxygen distances ranging from 2.13 to 2.35 Å (Figure 2). Only one protein residue, Asp145, participates in coordination, and water molecules (W1−W5) occupy the five remaining positions. The coordinating oxygen atoms interact with protein atoms, substrate atoms (see below), and other water molecules. W1 hydrogen bonds to Glu179* and a ΨMP phosphate oxygen atom. W2 hydrogen bonds to His137 and a ΨMP phosphate oxygen atom. W3 hydrogen bonds to Asp145 and the carbonyl oxygen atom of Gly266. W4 hydrogen bonds to Glu176* and Glu179*. W5 hydrogen bonds to a water molecule in the second sphere (W11) and a water molecule (W7) that bridges to the ΨMP phosphate. The water molecules directly involved in Mn(II) interactions are involved in additional hydrogen bonding interactions that extend into the remainder of the active site.

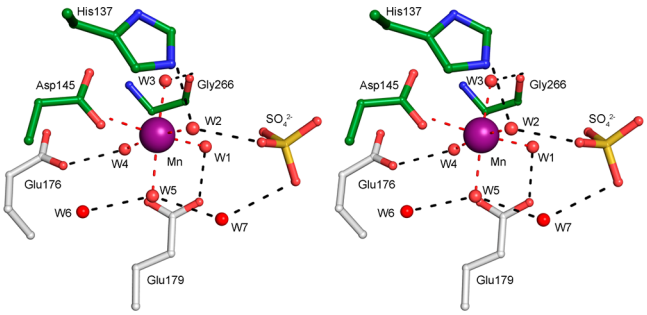

Figure 2. Stereoview of the Mn(II) binding site. Water molecules and protein atoms in the first and second coordination spheres are shown. The sulfate ion results from the crystallization conditions and occupies the phosphate binding site.

ΨMP Glycosidase Active Site. The active site, as defined by the structure of the K166A−ΨMP complex, is located in a cleft formed by helices α12 and α13 and the loops following strands β2, β7, and β8 (Figure 3A,B). The ΨMP ribose is in a C3′-*endo* conformation; the glycosidic torsion angle is *anti*, and the C4′−C5′ bond is in a *gauche*, *trans* conformation. Including the Mn(II) coordination sphere, the active site contains 19 well-ordered water molecules that are present in all three protomers. ΨMP is surrounded by 15 of the water molecules, and these mediate many of the active site contacts with the protein. One of the ΨMP phosphate oxygen atoms forms hydrogen bonds with W1 from the Mn(II) coordination sphere, Lys93, and water molecule W11. A second phosphate oxygen atom forms hydrogen bonds with W2 from the Mn(II) coordination sphere, Ser147, and water molecule W10. The third phosphate oxygen atom forms hydrogen bonds with three water molecules (W7−W9), which interact through multiple contacts with the protein (Ser95, Thr112, Ala148 NH, Asp149, and Glu179*). The ribose O2′-hydroxyl group hydrogen bonds to Glu31; the O3′-hydroxyl group hydrogen bonds to Asp149 and the Val113 amide group, while O4′ hydrogen bonds with water molecule W12, which in turn hydrogen bonds to Lys93 and W19.

The ΨMP uracil forms no direct hydrogen bonds with protein residues; however, N1, O2, N3, and O4 form hydrogen bonds with five water molecules. One water molecule (W14) hydrogen bonds to N1 and W15 and forms a bridge to the ΨMP phosphate through two additional water molecules (W10 and W13). The second water molecule (W16) hydrogen bonds to O2, the side chain of Asn289, W17, and W18, which is positioned over the center of the uracil ring and hydrogen bonds to the amide nitrogen and carbonyl oxygen atoms of Gly132. The third water molecule (W15) also hydrogen bonds to O2, the amide nitrogen atom of Ala166, and W14. The fourth water molecule (W18) hydrogen bonds to N3, the carbonyl oxygen atom of Gly38, and the side chain of Asn289. The fifth water molecule (W19) hydrogen bonds to O4, the carbonyl oxygen atom of His37, and an additional water molecule (W12), which hydrogen bonds to O4′ of ΨMP and Lys93.

Structure of the ΨMP Glycosidase−Ring-Opened Ribose ΨMP Adduct. The structure of ΨMP glycosidase cocrystallized with R5P and uracil shows ring-opened ribose ΨMP covalently attached to Lys166. Ring opening and closing are correlated with an approximately 90° rotation and a 2 Å shift of the uracil (Figure 4A,B), thus occupying a binding site different from that of the K166A−ΨMP complex. In this binding site, O2 forms a hydrogen bond with Asn289. The ring-opened ribose retains hydrogen bonds between the 2′-hydroxyl group and Glu31 and between the 3′-hydroxyl group and Asp149; however, the hydrogen bond to O3′ requires a rotation of the Glu31 carboxylate about the Cγ−Cδ bond compared to the ΨMP complex. The phosphate group maintains the same position as in the K166A−ΨMP structure and forms hydrogen bonds with Lys93, Ser147, W1, W2, and W7−W11. The water molecules near the uracil are not well-defined, possibly because of the lower resolution (2.5 Å) of this structure.

Structure of the ΨMP Glycosidase−R5P Adduct. Crystals of ΨMP treated with R5P show a structure in which

dx.doi.org/10.1021/bi3006829 | *Biochemistry* 2012, 51, 9245−9255

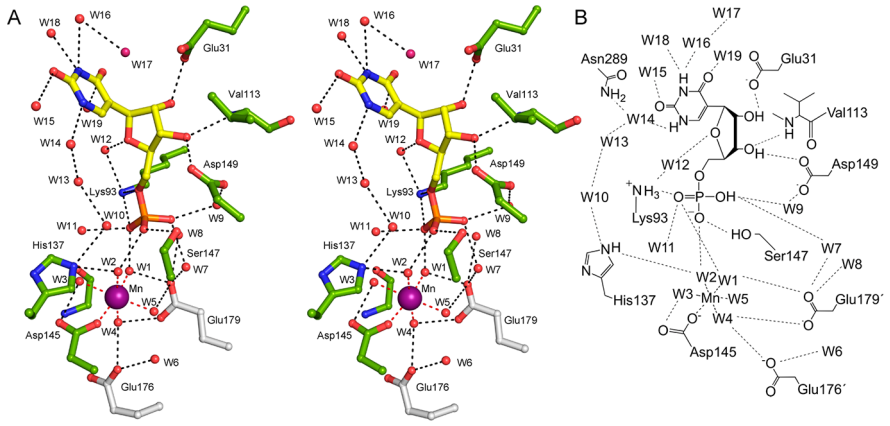

Figure 3. ΨMP glycosidase active site. (A) Stereoview of the K166A−ΨMP active site. ΨMP was observed in the active site upon cocrystallization of K166A with either ΨMP or R5P and uracil. ΨMP and Mn(II) form extensive hydrogen bond connections with the active site residues and water molecules. The dashed lines represent interactions provided by the residues that make up the hydrogen bond network. (B) Schematic diagram of the K166A−ΨMP complex.

the R5P is in the ring-opened form and is covalently attached to Lys166 via an imine. The R5P superimposes closely with the ring-opened ribose in the ΨMP adduct and forms hydrogen bonds between the 2-hydroxyl group and Glu31 and between the 3-hydroxyl group and Asp149 (Figure 4B,C). The phosphate binding site is essentially the same as for the previous complexes. Water molecules in the uracil binding site are less ordered and more variable from protomer to protomer compared to those of the K166A−ΨMP complex.

Detection of a Lys166 R5P Covalent Adduct by Mass Spectrometry. The mass of wild-type ΨMP glycosidase was determined to be 35453.4 Da by ICR-MS analysis (Figure 5A). The mass of the reduced R5P complex was 35668.4 Da, corresponding to a mass increase of 215 Da. This is consistent with a doubly protonated reduced R5P-derived imine (214 Da). Adduct formation was not observed when only uracil was incubated with ΨMP glycosidase.

The site of imine formation was identified by trypsin digestion of the reduced ΨMP glycosidase R5P adduct (Figure 5B−E). Trypsin cleaves after lysine and arginine residues, and lysine modification blocks the cleavage reaction. Trypsin digestion of the unmodified enzyme yielded the GAEHTFDISADLQELANTNVTVVCAGA**K** peptide (mass of 2930.4079 Da, amino acids 139−166). For glycosidase incubated with R5P, trypsin digestion yielded the GAEHTFDISADLQELANTNVTVVCAGA**K**SILDLGLTTEYLETFGVPLIGYQTK peptide (mass of 5896.8759 Da, amino acids 139−191). This demonstrates that Lys166 is the R5P-modified residue. This was confirmed by similar MS analysis of the K166A mutant for which no mass increase was observed for the R5P-treated sample.

Steady State Kinetics of EcΨMP Glycosidase and Its Mutants. Steady state kinetic parameters were determined by measuring the production of ΨMP during the reverse reaction while varying the uracil concentration (Figure 1A of the Supporting Information). Michaelis−Menten analysis of the native enzyme indicated a K_m value of 169.6 μM for uracil and a k_{cat} of 3.74 s^{-1}. This corresponds to a catalytic efficiency, k_{cat}/K_m, of 22 × 10^3 M^{-1} s^{-1}.

Steady state kinetic parameters were also determined for the active site mutants E31A, K93A, K166A, and N289A (Table 2) (Figure 1 of the Supporting Information). The activity of D149A was below the detection limit even at an enzyme concentration as high as 100 μM. K93A has a higher K_m value than the wild-type enzyme. E31A, K93A, K166A, and N289A have significantly lower k_{cat} values, with E31A and K166A showing the largest effects.

DISCUSSION

Comparison with Other Protein Structures. A structural similarity search for ΨMP glycosidase was performed using DALI.[35] Not surprisingly, PDB entry 1VKM, which was used as the search model during molecular replacement, showed the highest degree of similarity with a Z score of 42.2 (39% identical sequence). PDB entry 1VKM was originally reported by a structural genomics group to be an indigoidine synthase (IndA)-like protein from *T. maritima*.[26] Subsequent biochemical studies conclusively demonstrated that this protein is a ΨMP glycosidase.[4] The structure of the EcΨMP glycosidase is trimeric. The structure of ΨMP glycosidase from *T. maritima* (TmΨMP glycosidase) is hexameric in the crystal structure; however, this hexamer is an artifact resulting from face-to-face packing of two trimers, in which pairs of N-terminal His tags are joined by metal ions. Each of the TmΨMP glycosidase trimers is homologous to the EcΨMP glycosidase trimer, and both enzymes contain a bound Mn(II).

TmΨMP glycosidase was reported to be copurified with an unknown bound ligand that resembled a ring-opened sugar phosphate.[26] Motivated by our structural results, we reexamined this electron density and found that in some protomers a ring-opened R5P covalently attached to a lysine residue (equivalent to Lys166 in EcΨMP glycosidase) provided a good fit to the electron density while in others the ribose was in the ring-opened form but did not appear to be covalently attached.

Mechanistic Implications. The mechanism of pseudouridine synthase has been extensively studied and is outlined in Figure 6.[36] The microscopic reverse of this reaction would seem to be a reasonable starting hypothesis for the reaction catalyzed by ΨMP glycosidase. In this proposal, tautomerization of ΨMP **2** to give **9** followed by C glycosyl bond cleavage and trapping of the resulting oxocarbenium ion would give **7** and **8**. Hydrolysis of **8** and protonation of **7** would complete the reaction

Our structural studies identified four snapshots of the EcΨMP glycosidase reaction coordinate. Wild-type EcΨMP

dx.doi.org/10.1021/bi3006829 | *Biochemistry* 2012, 51, 9245−9255

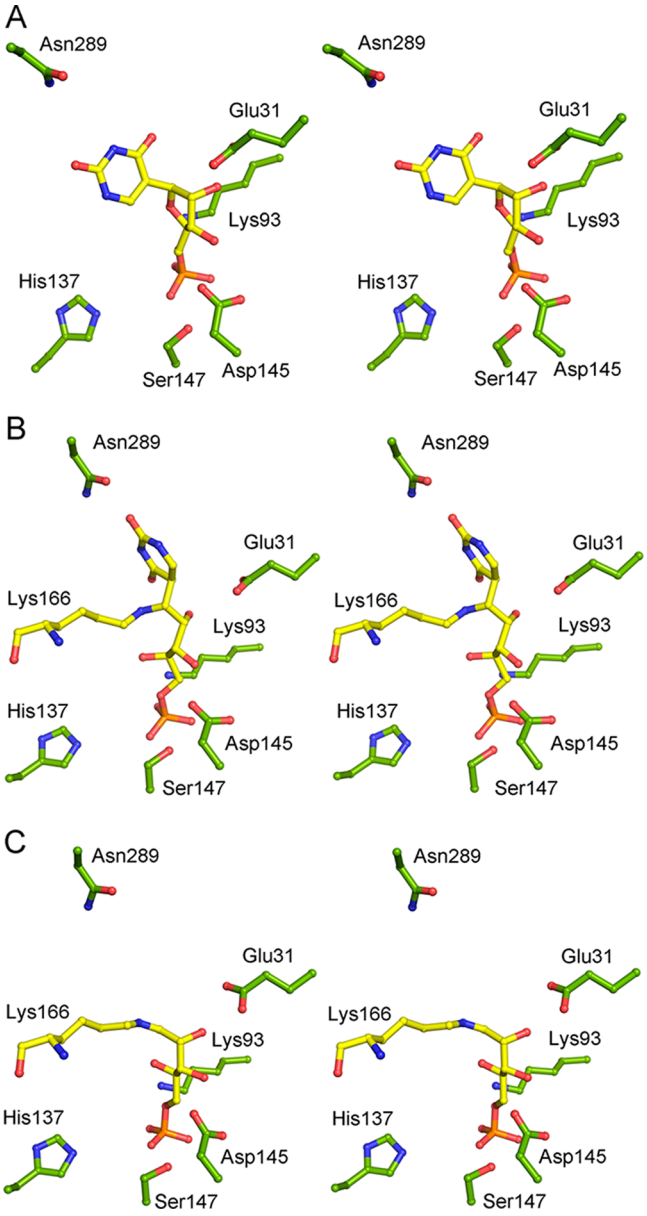

Figure 4. Comparison of ΨMP glycosidase complexes. (A) Stereoview of the K166A−ΨMP complex. (B) Stereoview of the ΨMP glycosidase−ring-opened ribose ΨMP adduct. (C) Stereoview of the ΨMP glycosidase−R5P adduct. Protein carbon atoms are colored green; ligand carbon atoms are colored yellow.

showed the unliganded state, although a sulfate ion from the crystallization solutions occupied the phosphate binding site. Incubation of the K166A mutant with R5P and uracil resulted in a structure with the substrate ΨMP bound in the active site. Native EcΨMP glycosidase incubated with R5P and uracil showed an intermediate in which ring-opened ribose ΨMP is covalently attached to Lys166. Finally, EcΨMP glycosidase incubated with R5P alone resulted in a structure with ring-opened R5P attached to Lys166. The last structure is similar to that of the 1VKM complex reported to contain an unknown ligand.[26] This series of structures demonstrated that the ΨMP glycosidase-catalyzed reaction occurs by a mechanism that is significantly different from the microscopic reverse of the pseudouridine synthase mechanism.

An alternative mechanistic proposal is outlined in Figure 7. Ring opening of the ΨMP ribose gives **10**. This reaction requires acid−base catalysis. As no amino acids are apparent in the structure for this role (Figure 3), the ring-opening reaction probably occurs by a water-mediated protonation−deprotonation reaction. The conformation of the C glycosidic bond is reasonable for a concerted process (the C6−C5−C1−O4a dihedral angle is 50°, while the optimal angle would be 90°). Related ribose ring-opening reactions are catalyzed by GTP cyclohydrolase.[37] Following ribose ring opening, Lys166 undergoes a conjugate addition to the C−C double bond of **10** to give **11** with the proton coming from Glu31. Subsequent cleavage of the C−C glycosidic bond by a retroaldol-type reaction releases the uracil anion, which is stabilized by hydrogen bonding of N1 to the hydroxyl of Thr130 and the amide NH of Gly131 and Gly132. Surprisingly, there are no stabilizing hydrogen bonds to the C2 or C4 carbonyl oxygen atoms of uracil. Hydrolysis of imine **12** gives **13**, which will then cyclize to **3**. In addition to the structures, the covalent linkage between Lys166 and the substrate is supported by the characterization of the R5P Lys166 imine by mass spectrometry. An alternative mechanism in which Lys166 displaces the pyrimidine from the ribose, as found, for example, in 8-oxoguanine DNA glycosylase,[38] is unlikely. Lysine 166, modeled into the structure of the enzyme ΨMP complex, is not suitably positioned for direct base displacement, and the structure of the ring-opened ribose ΨMP complex is not consistent with this mechanism. The structure of UrdGT2, with the substrates modeled into the active site, suggests that this C−C glycosyl transferase does not use an imine intermediate.[24] Our analysis suggests that ΨMP glycosidase may use a new glycosidase mechanism.

This mechanistic proposal allows us to suggest testable functions for the active site residues. Lys166 plays a key role in facilitating the C glycosyl bond cleavage reaction, and as expected, the k_{cat} value of the K166A mutant is 2900-fold lower than that of the wild type, with no change in K_m. It is interesting that low levels of catalytic activity are observed for this mutant, suggesting that water can replace lysine in the mutant. Glu31 is likely to be the proton source for the lysine conjugate addition reaction (**10** to **11** in Figure 7). Consistent with this role, the k_{cat} value of the E31A mutant is 7500-fold lower than that of the wild type, with little change in K_m. Lys93 contributes one of several interactions involved in phosphate binding. The k_{cat} value of the K93A mutant is 17-fold lower than that of the wild type, with only a modest increase in K_m. Asn289 hydrogen bonds to two water molecules that are in turn hydrogen bonded to the C2 carbonyl and to N3. These interactions stabilize the negative charge on the uracil in the conversion of **11** to **12** and **4**. Consequently, the k_{cat} value of the N289A mutant is 17-fold lower than that of the wild type, with a small increase in K_m. Asp149 forms a hydrogen bond to the substrate C3′ alcohol. We would therefore expect that the activity of the D149A mutant would be comparable to that of the wild type, which is inconsistent with our finding that it shows no detectable activity. One possibility is that the D149A mutant has misfolded; however, CD spectra of the wild type and D149A are nearly identical (unpublished experiments). Another possibility is that Asp149 serves indirectly as an acid and/or base through a charged network.

Role of the Hydrated Metal Binding Site. Both EcΨMP glycosidase and TmΨMP glycosidase contain heavily hydrated, octahedrally coordinated Mn(II) ions in which the ligands are

dx.doi.org/10.1021/bi3006829 | *Biochemistry* 2012, 51, 9245−9255

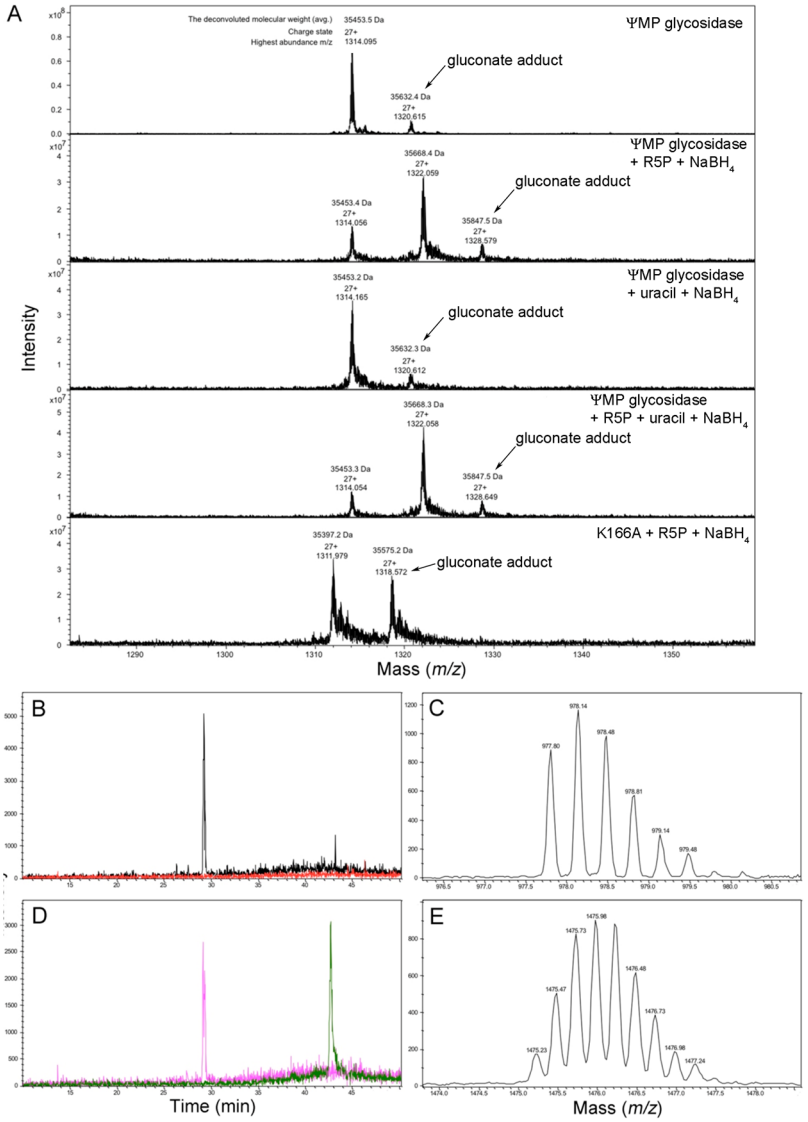

Figure 5. Analysis of the R5P adduct by mass spectrometry. (A) ICR-MS data for the identification of the borohydride-reduced ΨMP glycosidase−R5P adduct. The observed 179 Da adduct corresponds to enzyme gluconoylation.[39] (B) MS chromatograms of the control sample. The black trace corresponds to data for the unmodified peptide, while the red trace corresponds to data for the R5P-bound peptide, which is not seen in the ΨMP glycosidase control. (C) Triply charged state of the unmodified peptide in the control ΨMP glycosidase sample. (D) MS chromatograms of the reduced ΨMP glycosidase−/R5P adduct. The pink trace corresponds to data for the unmodified peptide, while the green trace corresponds to data for the R5P-bound modified peptide. (E) Quadruply charged state of the R5P-bound modified peptide in the reduced ΨMP glycosidase−R5P adduct.

Table 2. Steady State Kinetic Parameters for ΨMP Glycosidase and Mutants[a]

Enzyme	k_{cat} (s^{-1})	K_m (μM)	k_{cat}/K_m (M^{-1} s^{-1})
ΨMP glycosidase	3.74 ± 0.14	169.6 ± 21.6	(22 ± 3.6) × 10^3
K166A	0.0013 ± 0.00005	162.4 ± 23.5	8 ± 1.5
E31A	0.0005 ± 0.00005	191 ± 39.3	2.6 ± 0.8
K93A	0.22 ± 0.007	300.5 ± 21.8	(0.73 ± 0.076) × 10^3
N289A	0.23 ± 0.007	214.2 ± 18.7	(1.1 ± 0.13) × 10^3
D149A	NA[b]	NA[b]	NA[b]

[a]All the kinetic parameters were determined by monitoring the conversion of uracil to ΨMP at a saturating R5P concentration; k_{cat} and K_m are determined for uracil. [b]No activity was detected under standard assay conditions.

an aspartate side chain and five water molecules. In addition, the water molecules in the second sphere (W6−W9) are also present in both structures, and all side chains in the second sphere are conserved, including Glu176 and Glu179 from the neighboring protomer. This heavily hydrated metal binding site is unusual and likely plays a role in anchoring the ΨMP phosphate. Two phosphate oxygen atoms form hydrogen bonds to W1 and W2, which are in the Mn(II) coordination sphere. The phosphate group also hydrogen bonds to Ser147 and Lys93, which are conserved in both structures. While the

dx.doi.org/10.1021/bi3006829 | Biochemistry 2012, 51, 9245−9255

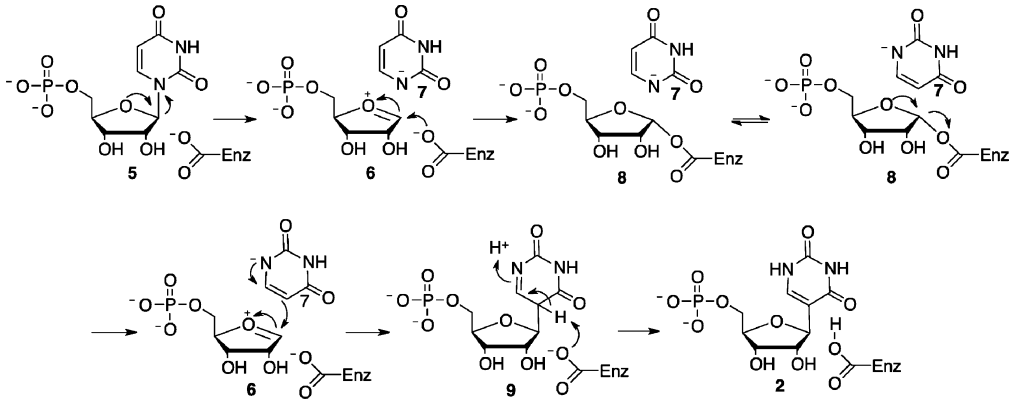

Figure 6. Mechanism of pseudouridine formation. This mechanism suggested a plausible starting mechanistic hypothesis for ΨMP glycosidase.

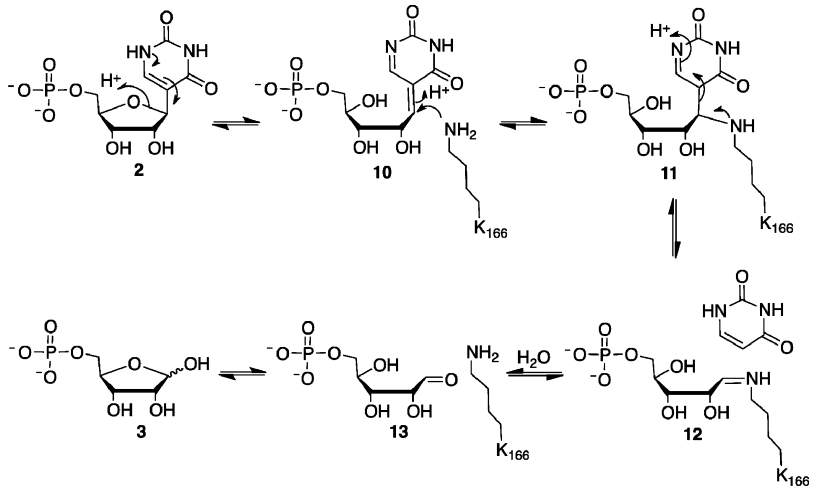

Figure 7. Mechanistic proposal for ΨMP glycosidase.

ribose and uracil both undergo movement during catalysis, the phosphate remains in the same position, with no hydrogen bonding changes. ΨMP glycosidase shows the highest activities with Fe(II), Co(II), and Mn(II), while Zn(II) and, to a lesser extent, Ni(II) were inhibitory.[4] These observations suggest that the ionic radius of the metal ion may play a role in properly positioning the substrate.

Role of Conformational Changes in Catalysis. Both the protein and substrate undergo conformational changes during catalysis. The uracil undergoes a 90° rotation and a 2 Å shift after ring opening and Lys166 adduct formation. In the glycosidase ΨMP complex, uracil forms no hydrogen bonds with protein atoms; however, after shifting position, uracil hydrogen bonds through O2 to Asn289, which is located at the opposite end of the active site relative to the phosphate. Repositioning of the uracil also places N1 near the amide nitrogen atoms of Gly131 and Gly132, which are absolutely conserved. Heavy reliance in the binding site on water-mediated interactions is consistent with the need for major repositioning of an intermediate during catalysis.

Comparison of the 12 protomers (three each from four structures) suggests that conformational changes in the protein are also involved in catalysis. The largest differences occur in helices α11 and α12 with rmsds ranging from 1.5 to 7.0 Å for the pairwise comparisons. At one extreme, these residues insert into the active site, acting as a gate. At the other extreme, these residues are extended from the active site making room for substrate binding. In all of the structures, these residues tend to show weaker electron density and higher *B* factors. A second region of structural variation occurs in residues 130−150 (α7 and α8) and 162−200 (helix α9 and β9) with rmsds ranging from 1.5 to 5.0 Å. This region contains 14 of 17 absolutely conserved residues. While crystal packing may also play a role in the variation among protomers, the differences are consistent with gating of the active site and positioning of catalytically important residues.

■ CONCLUSION

The ΨMP glycosidase complexes described in this paper give four snapshots of the reaction coordinate and provide key structural insights into the enzymatic hydrolysis of C-glycosides. Most glycosidases utilize a dissociative mechanism to reversibly cleave C−N and C−O glycosidic bonds. In contrast, the structural and biochemical studies reported here demonstrate that ΨMP glycosidase utilizes a mechanism involving ribose ring opening and subsequent covalent linkage between C1′ and an active site lysine, thus setting the stage for a facile C glycosyl bond fragmentation by a novel retroaldol-type mechanism.

■ ASSOCIATED CONTENT

Supporting Information

Michaelis−Menten plots for ΨMP glycosidase and its mutants (Figure 1) and primers used for the mutations (Table 1). This

dx.doi.org/10.1021/bi3006829 | *Biochemistry* 2012, 51, 9245−9255

material is available free of charge via the Internet at http://pubs.acs.org.

Accession Codes

Coordinates of ΨMP glycosidase, the R5P adduct, the ΨMP covalent adduct, and the K166A−ΨMP complex have been deposited as Protein Data Bank entries 4GIJ, 4GIK, 4GIL, and 4GIM, respectively.

AUTHOR INFORMATION

Corresponding Author

*Department of Chemistry and Chemical Biology, Cornell University, Ithaca, NY 14853. Telephone: (607) 255-7961. Fax: (607) 255-1227. E-mail: see3@cornell.edu (S.E.E.) or begley@mail.chem.tamu.edu (T.P.B.).

Funding

This work was supported by National Institutes of Health (NIH) Grant GM73220 (to S.E.E.) and the Robert A. Welch Foundation (Grant A-0034 to T.P.B.). This work is based upon research conducted at the Advanced Photon Source on the Northeastern Collaborative Access Team beamlines, which are supported by Grant GM103403 from the National Institute of General Medical Sciences of the National Institutes of Health. Use of the Advanced Photon Source is supported by the U.S. Department of Energy, Office of Basic Energy Sciences, under Contract DE-AC02-06CH11357. MacCHESS is supported by NIH Grant RR01646 at the Cornell High Energy Synchrotron Source.

Notes

The authors declare no competing financial interest.

ACKNOWLEDGMENTS

We thank Dr. Cynthia Kinsland for cloning ΨMP glycosidase, Leslie Kinsland for assistance in preparing the manuscript, and the staff of the NE-CAT at the APS and the staff of the Cornell High Energy Synchrotron Source for assistance with data collection. We thank Drs. David Russell, Pei-Jing Pai, and Nathaniel F. Zinnel of the Laboratory for Biological Mass Spectrometry at Texas A&M University for the mass spectra of the native and ribose-modified native enzyme. We thank Tom Payne and Dr. Brian Crane for CD spectra of wild-type ΨMP glycosidase and the D149A mutant.

ABBREVIATIONS

TCEP, tris(2-carboxyethyl)phosphine; LB, Luria-Bertani; Ψ, pseudouridine; ΨMP, pseudouridine 5′-monophosphate; R5P, ribose 5-phosphate; rmsd, root-mean-square deviation; Tris, tris(hydroxymethyl)aminomethane; EcΨMP glycosidase, *E. coli* ΨMP glycosidase; TmΨMP glycosidase, *T. maritima* ΨMP glycosidase; NE-CAT, Northeast Collaborative Access Team; APS, Advanced Photon Source.

REFERENCES

(1) Charette, M., and Gray, M. W. (2000) Pseudouridine in RNA: What, Where, How, and Why. *IUBMB Life 49*, 341−351.

(2) Hoang, C., and Ferré-D'Amaré, A. R. (2001) Cocrystal Structure of a tRNA [Psi]55 Pseudouridine Synthase: Nucleotide Flipping by an RNA-Modifying Enzyme. *Cell 107*, 929−939.

(3) Uliel, S., Liang, X.-h., Unger, R., and Michaeli, S. (2004) Small nucleolar RNAs that guide modification in trypanosomatids: Repertoire, targets, genome organisation, and unique functions. *Int. J. Parasitol. 34*, 445−454.

(4) Preumont, A., Snoussi, K., Stroobant, V., Collet, J. F., and Van Schaftingen, E. (2008) Molecular identification of pseudouridine-metabolizing enzymes. *J. Biol. Chem. 283*, 25238−25246.

(5) Feng, B., Zheng, M. H., Zheng, Y. F., Lu, A. G., Li, J. W., Wang, M. L., Ma, J. J., Xu, G. W., Liu, B. Y., and Zhu, Z. G. (2005) Normal and modified urinary nucleosides represent novel biomarkers for colorectal cancer diagnosis and surgery monitoring. *J. Gastroenterol. Hepatol. 20*, 1913−1919.

(6) Bililign, T., Griffith, B. R., and Thorson, J. S. (2005) Structure, activity, synthesis and biosynthesis of aryl-C-glycosides. *Nat. Prod. Rep. 22*, 742−760.

(7) Gopaul, D. N., Meyer, S. L., Degano, M., Sacchettini, J. C., and Schramm, V. L. (1996) Inosine-uridine nucleoside hydrolase from *Crithidia fasciculata*. Genetic characterization, crystallization, and identification of histidine 241 as a catalytic site residue. *Biochemistry 35*, 5963−5970.

(8) Duerre, J. A. (1962) Hydrolytic Nucleosidase Acting on *S*-Adenosylhomocysteine and on 5′-Methylthioadenosine. *J. Biol. Chem. 237*, 3737.

(9) Hurwitz, J., Heppel, L. A., and Horecker, B. L. (1957) The Enzymatic Cleavage of Adenylic Acid to Adenine and Ribose 5-Phosphate. *J. Biol. Chem. 226*, 525−540.

(10) Pugmire, M. J., and Ealick, S. E. (1998) The crystal structure of pyrimidine nucleoside phosphorylase in a closed conformation. *Structure 6*, 1467−1479.

(11) Flaks, J. G., Erwin, M. J., and Buchanan, J. M. (1957) Biosynthesis of the Purines. 16. The Synthesis of Adenosine 5′-Phosphate and 5-Amino-4-Imidazolecarboxamide Ribotide by a Nucleotide Pyrophosphorylase. *J. Biol. Chem. 228*, 201−213.

(12) Olsen, A. S., and Milman, G. (1974) Chinese-Hamster Hypoxanthine-Guanine Phosphoribosyltransferase: Purification, Structural, and Catalytic Properties. *J. Biol. Chem. 249*, 4030−4037.

(13) Short, S. A., Armstrong, S. R., Ealick, S. E., and Porter, D. J. T. (1996) Active site amino acids that participate in the catalytic mechanism of nucleoside 2′-deoxyribosyltransferase. *J. Biol. Chem. 271*, 4978−4987.

(14) Fromme, J. C., and Verdine, G. L. (2003) Structure of a trapped endonuclease III-DNA covalent intermediate. *EMBO J. 22*, 3461−3471.

(15) Lairson, L. L., Henrissat, B., Davies, G. J., and Withers, S. G. (2008) Glycosyltransferases: Structures, functions, and mechanisms. *Annu. Rev. Biochem. 77*, 521−555.

(16) Kharel, M. K., Pahari, P., Shepherd, M. D., Tibrewal, N., Nybo, S. E., Shaaban, K. A., and Rohr, J. (2012) Angucyclines. Biosynthesis, mode-of-action, new natural products, and synthesis. *Nat. Prod. Rep. 29*, 264−325.

(17) Nolan, E. M., Fischbach, M. A., Koglin, A., and Walsh, C. T. (2007) Biosynthetic Tailoring of Microcin E492m: Post-translational Modification Affords an Antibacterial Siderophore-Peptide Conjugate. *J. Am. Chem. Soc. 129*, 14336−14347.

(18) Fischbach, M. A., Lin, H., Liu, D. R., and Walsh, C. T. (2005) In vitro characterization of IroB, a pathogen-associated C-glycosyltransferase. *Proc. Natl. Acad. Sci. U.S.A. 102*, 571−576.

(19) Brazier-Hicks, M., Evans, K. M., Gershater, M. C., Puschmann, H., Steel, P. G., and Edwards, R. (2009) The C-glycosylation of flavonoids in cereals. *J. Biol. Chem. 284*, 17926−17934.

(20) Siitonen, V., Claesson, M., Patrikainen, P., Aromaa, M., Maentsaelae, P., Schneider, G., and Metsae-Ketelae, M. (2012) Identification of late-stage glycosylation steps in the biosynthetic pathway of the anthracycline nogalamycin. *ChemBioChem 13*, 120−128.

(21) Oja, T., Klika, K. D., Appassamy, L., Sinkkonen, J., Mantsala, P., Niemi, J., and Metsa-Ketela, M. (2012) Biosynthetic pathway toward carbohydrate-like moieties of alnumycins contains unusual steps for C-C bond formation and cleavage. *Proc. Natl. Acad. Sci. U.S.A. 109*, 6024−6029.

(22) Dumitru, R. V., and Ragsdale, S. W. (2004) Mechanism of 4-(β-D-Ribofuranosyl)aminobenzene 5′-Phosphate Synthase, a Key Enzyme

in the Methanopterin Biosynthetic Pathway. *J. Biol. Chem. 279*, 39389−39395.
(23) White, R. H. (2011) The conversion of a phenol to an aniline occurs in the biochemical formation of the 1-(4-aminophenyl)-1-deoxy-D-ribitol moiety in methanopterin. *Biochemistry 50*, 6041−6052.
(24) Mittler, M., Bechthold, A., and Schulz, G. E. (2007) Structure and Action of the C-C Bond-forming Glycosyltransferase UrdGT2 Involved in the Biosynthesis of the Antibiotic Urdamycin. *J. Mol. Biol. 372*, 67−76.
(25) Chang, A., Singh, S., Phillips, G. N., Jr., and Thorson, J. S. (2011) Glycosyltransferase structural biology and its role in the design of catalysts for glycosylation. *Curr. Opin. Biotechnol. 22*, 800−808.
(26) Levin, I., Miller, M. D., Schwarzenbacher, R., McMullan, D., Abdubek, P., Ambing, E., Biorac, T., Cambell, J., Canaves, J. M., Chiu, H. J., Deacon, A. M., DiDonato, M., Elsliger, M. A., Godzik, A., Grittini, C., Grzechnik, S. K., Hale, J., Hampton, E., Han, G. W., Haugen, J., Hornsby, M., Jaroszewski, L., Karlak, C., Klock, H. E., Koesema, E., Kreusch, A., Kuhn, P., Lesley, S. A., Morse, A., Moy, K., Nigoghossian, E., Ouyang, J., Page, R., Quijano, K., Reyes, R., Robb, A., Sims, E., Spraggon, G., Stevens, R. C., van den Bedem, H., Velasquez, J., Vincent, J., Wang, X., West, B., Wolf, G., Xu, Q., Zagnitko, O., Hodgson, K. O., Wooley, J., and Wilson, I. A. (2005) Crystal structure of an indigoidine synthase A (IndA)-like protein (TM1464) from *Thermotoga maritima* at 1.90 Å resolution reveals a new fold. *Proteins 59*, 864−868.
(27) Ausubel, F. M., and Brent, F. (1987) *Current Protocols in Molecular Biology*, John Wiley and Sons, New York.
(28) Vita, A., Huang, C. Y., and Magni, G. (1983) Uridine phosphorylase from *Escherichia coli* B.: Kinetic studies on the mechanism of catalysis. *Arch. Biochem. Biophys. 226*, 687−692.
(29) Otwinowski, Z., and Minor, W. (1997) Processing of X-ray diffraction data collected in oscillation mode. *Methods Enzymol. 276*, 307−326.
(30) Vagin, A., and Teplyakov, A. (2000) An approach to multi-copy search in molecular replacement. *Acta Crystallogr. D56*, 1622−1624.
(31) Stein, N. (2008) CHAINSAW: A program for mutating PDB files used as templates in molecular replacement. *J. Appl. Crystallogr. 41*, 641−643.
(32) Emsley, P., and Cowtan, K. (2004) Coot: Model-building tools for molecular graphics. *Acta Crystallogr. D60*, 2126−2132.
(33) Murshudov, G. N., Vagin, A. A., Lebedev, A., Wilson, K. S., and Dodson, E. J. (1999) Efficient anisotropic refinement of macromolecular structures using FFT. *Acta Crystallogr. D55*, 247−255.
(34) Adams, P. D., Grosse-Kunstleve, R. W., Hung, L. W., Ioerger, T. R., McCoy, A. J., Moriarty, N. W., Read, R. J., Sacchettini, J. C., Sauter, N. K., and Terwilliger, T. C. (2002) PHENIX: Building new software for automated crystallographic structure determination. *Acta Crystallogr. D58*, 1948−1954.
(35) Holm, L., and Rosenstrom, P. (2010) Dali server: Conservation mapping in 3D. *Nucleic Acids Res. 38* (Suppl.), W545−W549.
(36) Miracco, E. J., and Mueller, E. G. (2011) The products of 5-fluorouridine by the action of the pseudouridine synthase TruB disfavor one mechanism and suggest another. *J. Am. Chem. Soc. 133*, 11826−11829.
(37) Rebelo, J., Auerbach, G., Bader, G., Bracher, A., Nar, H., Hosl, C., Schramek, N., Kaiser, J., Bacher, A., Huber, R., and Fischer, M. (2003) Biosynthesis of Pteridines. Reaction Mechanism of GTP Cyclohydrolase I. *J. Mol. Biol. 326*, 503−516.
(38) Chung, S. J., and Verdine, G. L. (2004) Structures of End Products Resulting from Lesion Processing by a DNA Glycosylase/Lyase. *Chem. Biol. 11*, 1643−1649.
(39) Geoghegan, K. F., Dixon, H. B., Rosner, P. J., Hoth, L. R., Lanzetti, A. J., Borzilleri, K. A., Marr, E. S., Pezzullo, L. H., Martin, L. B., LeMotte, P. K., McColl, A. S., Kamath, A. V., and Stroh, J. G. (1999) Spontaneous α-N-6-phosphogluconoylation of a "His tag" in *Escherichia coli*: The cause of extra mass of 258 or 178 Da in fusion proteins. *Anal. Biochem. 267*, 169−184.